Broad-Band Diode Phase Shifters

ROBERT V. GARVER, SENIOR MEMBER, IEEE

Abstract—Design figures are presented for four types of diode phase shifters: switched line, reflection, loaded line, and a new type using lumped-element high-pass and low-pass circuits. Comparison of their bandwidths shows that most of them can work over an octave bandwidth.

Introduction

THREE TYPES of phase shifters are well known, switched line [1], [2], reflection [3], [4], and loaded line [5], [6]. Although many versions of these phase shifters have been designed, none of the designs has exploited the full bandwidth possibilities of these circuits. Most designs to date have a maximum bandwidth of about 10 percent, but most of the circuits have a maximum potential bandwidth of an octave. A new type of phase shifter [7], using lumped-element high-pass and low-pass circuits, has the potential of being smaller than the other types and of providing slightly greater bandwidth. The four types of phase shifters with their design equations are shown in Fig. 1.

The bandwidth specification depends on the system requirements. Broad-band phase shifters for phased array radars must provide a constant time delay, while broad-band phase shifters for serrodyne modulators or phase comparison networks should provide constant phase shift. The switched-line and reflection types of phase shifters are most suitable for constant time delay, while all four types can be made into constant phase-shift devices.

A. Switched-Line Phase Shifters

As shown in Fig. 1, the switched-line phase shifter uses two SPDT switches. The lower path has transmission length l, while the upper path has transmission length $l+\Delta l$. The upper path has a phase delay longer than the lower path given by

$$\Delta\phi = 2\pi\Delta l/\lambda. \tag{1}$$

1) Spacing l: The length l must be carefully selected to avoid phase errors and high or unbalanced insertion losses. Several attempts have been made to analyze these errors as a function of l [8]–[10]. The method of Wilkinson *et al.* [10] has proven to be the most exact and is described in this paper. It is demonstrated here that large errors occur when the effective length of an OFF path is $\lambda/2$ or multiples thereof. The effective length is the electrical length plus the equivalent length of the capacitive OFF diode switches.

Manuscript received June 21, 1971; revised October 6, 1971.
The author is with Harry Diamond Laboratories, Washington, D. C. 20438.

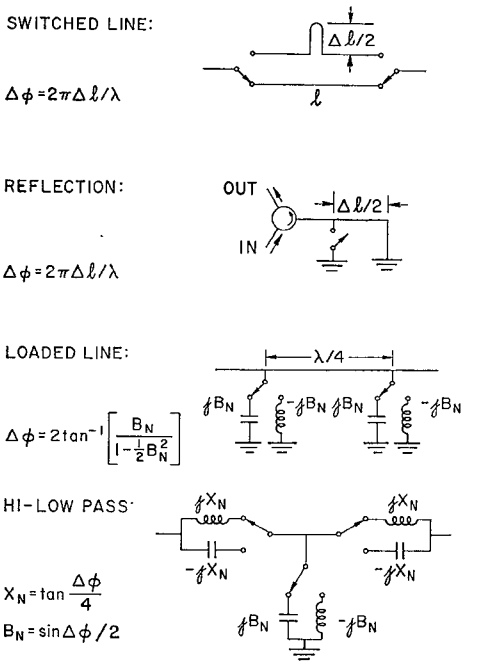

Fig. 1. Phase shifter circuits.

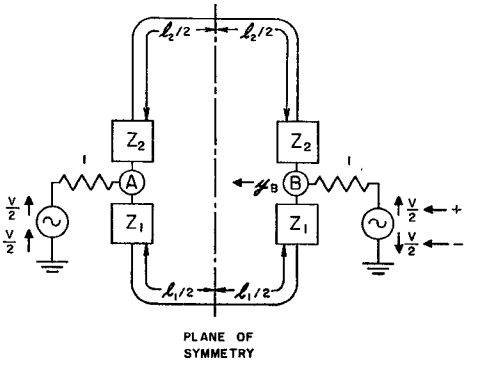

Fig. 2. Detailed equivalent circuit of the switched-line phase shifter.

These errors in phase and insertion loss may be calculated exactly using the circuit shown in Fig. 2. The superposition theorem is used to determine the voltage of B. All impedances are normalized to the generator impedance, which is also equal to all transmission line characteristic impedances. The upper generator voltage vectors are for even excitation of the circuit and are labeled +. For even excitation of the circuit, open-circuit terminations may be substituted at the plane of symmetry for the other half of the circuit. The lower generator voltage vectors are for odd excitation of the circuit and are labeled −. For odd excitation of the cir-

cuit, short-circuit terminations may be substituted at the plane of symmetry for the other half of the circuit.

For even excitation, the normalized admittance looking at the two transmission lines from point B, y_B^+ is given by

$$y_B^+ = \frac{1}{Z_1 - j\cot(2\pi l_1/2\lambda)} + \frac{1}{Z_2 - j\cot(2\pi l_2/2\lambda)}. \quad (2)$$

The normalized admittance for odd excitation y_B^- is given by

$$y_B^- = \frac{1}{Z_1 + j\tan(2\pi l_1/2\lambda)} + \frac{1}{Z_2 + j\tan(2\pi l_2/2\lambda)}. \quad (3)$$

The voltages at B, V_B are given by

$$V_B^+ = \frac{\frac{V}{2}\frac{1}{y_B^+}}{1 + \frac{1}{y_B^+}} \qquad V_B^- = \frac{-\frac{V}{2}\frac{1}{y_B^-}}{1 + \frac{1}{y_B^-}}. \quad (4)$$

The transmission term of the scattering matrix through the two-path network S_{21} is given by adding the voltages for even and odd excitation and dividing by the maximum delivered power voltage $V/2$. Then the left generator generates full voltage, and the right generator generates nothing.

$$S_{21} = \frac{V_B^+ + V_B^-}{V/2} = \frac{1}{y_B^+ + 1} - \frac{1}{y_B^- + 1} \quad (5)$$

$$S_{21} = \frac{1}{1 + \frac{1}{Z_1 - j\cot(\pi l_1/\lambda)} + \frac{1}{Z_2 - j\cot(\pi l_2/\lambda)}} - \frac{1}{1 + \frac{1}{Z_1 + j\tan(\pi l_1/\lambda)} + \frac{1}{Z_2 + j\tan(\pi l_2/\lambda)}}. \quad (6)$$

When $Z_1 = 0$

$$S_{21} = \frac{1}{1 + j\tan(\pi l_1/\lambda) + \frac{1}{Z_2 - j\cot(\pi l_2/\lambda)}} - \frac{1}{1 - j\cot(\pi l_1/\lambda) + \frac{1}{Z_2 + j\tan(\pi l_2/\lambda)}} \quad (7)$$

or when $Z_2 = 0$ all 1 and 2 subscripts are interchanged.

Integrated circuit switches can be made with very low insertion loss, but high isolation is difficult to obtain with single diodes. Thus the assumption that an ON diode can be represented by $Z = 0$ is quite reasonable. The errors for diodes providing capacitively limited SPST isolations of 10 and 20 dB and a resistively limited SPST isolation of 20 dB have been calculated. For the calculations, it is assumed that path l_1 is shorter than path l_2 and that path l_1 provides the reference phase. Thus path l_2 will provide a phase delay with respect to path l_1.

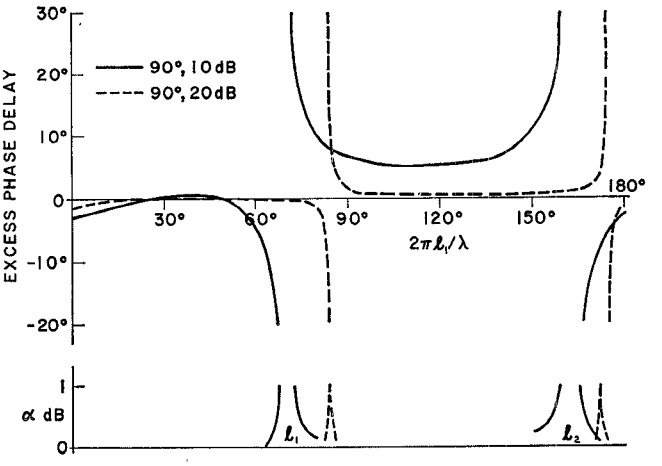

Fig. 3. Phase error and insertion loss of a 90° switched-line phase shifter.

When path l_2 is a half-wavelength longer than path l_1, the switching from path l_1 to path l_2 introduces an increased phase delay of 180°. Comparison of the phases of S_{21} in (7) for paths l_1 and l_2 indicates that the phase shift is exactly 180° for all values of l_1 as long as all four switching diodes are the same. There is no phase error. This holds true only for phase shifts of 180°. The insertion loss is also the same for all values of l_1 and for both phase states. An SPST resistive isolation of 20 dB gives a 0.5-dB insertion loss, a resistive 10 dB gives 1.8 dB, and a capacitive 10 dB gives 0.1 dB.

When path l_2 is a quarter-wavelength longer than path l_1, the phase shift is 90°. The error for various electrical lengths of path l_1 (path length expressed in degrees equals $2\pi l_1/\lambda$) is calculated using (7) and is plotted in Fig. 3. Errors become quite significant at two lengths of path l_1. At these two lengths the attenuation in one of the paths becomes infinite, and the phase error goes through a full 360°. The OFF diode capacitance adds to the effective length of the OFF path. When the effective length of the OFF path is a half-wavelength (or multiple thereof), it is resonant and the phases add up in such a manner as to reflect all incident power back to the generator. For example, 10-dB capacitive isolation (SPST) is given by a normalized series capacitive reactance of $X_N = -6$. This reactance corresponds to an open circuit line having an electrical length of 9.45°. One of these capacitors on each end of a line will add 18.9° to the effective electrical length of the line. Therefore, the line will have an effective electrical half-wavelength when it is 161.1° long. This length is the l_1 path that gives the insertion-loss spike and cycle or phase error for a capacitive 10-dB (SPST) isolation in Fig. 3. The other high-error length occurs when l_2 is a half-wavelength long, which occurs when the electrical length of l_1 is 161.1° $-90° = 71.1°$. The SPST 20-dB reactance is $X_N = -20$, which gives an effective electrical length of 2.88°, which

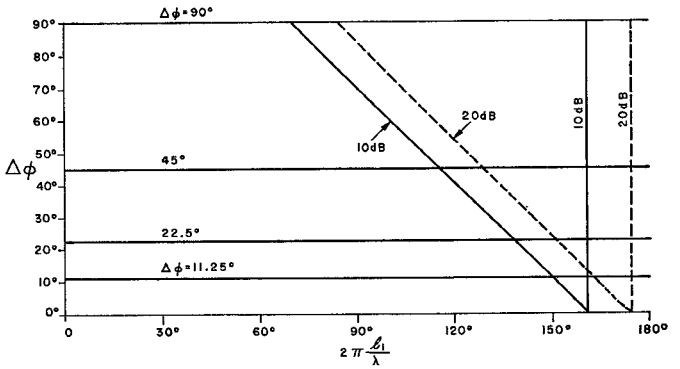

Fig. 4. Regions of maximum phase error and insertion loss for switched-line phase shifters.

in turn gives large errors when $2\pi l_1/\lambda$ is at 174.24° and 84.24°.

The curves of phase error are cyclic; they repeat every 180°. Even with the 10-dB isolation (SPST) diodes, phase errors are very low when $2\pi l_1/\lambda$ is between 20°and 50°. The insertion loss in this region for the 10-dB (SPST) switch is 0.1 dB in both phase states. The 20-dB switch gives far less insertion loss. (Insertion loss will be dominated by the resistive component of the OFF diode.) Higher isolation of the diodes only narrows the region of large phase error; the error persists.

Errors have been calculated for 45°, 22.5°, and 11.25°, all giving curves similar to Fig. 3 and all demonstrating high errors when the OFF path is $\lambda/2$. The calculated length of l_1 that causes large insertion loss and phase errors may be found easily by using Fig. 4.

The phase errors were also calculated for a resistively limited diode switch. The regions of small phase error are approximately the same as for reactively limited switches. The insertion loss in this region of small phase error was 0.5 dB for the 20-dB (SPST) switch and 1.8 dB for the 10-dB (SPST) switch. The insertion loss of path l_1 decreased at the first negative phase-error length and the insertion loss of path l_2 decreased at 0°. For small phase shifts, the insertion loss of each path approached zero at the appropriate lengths. In the region of small error, the insertion losses of both phase states were equal.

In general, the selection of $2\pi l_1/\lambda$ between 20° and 50° will insure that phase errors are a minimum, that the insertion losses in both phase states are equal, and that the phase shifter is not too large.

2) Insertion Loss: The insertion loss calculated earlier for the perfect ON diodes and resistive OFF diodes agrees exactly with the insertion loss [11] that would result from two resistors R_p shunting a transmission line Z_0:

$$\delta = 40 \log \left[1 + \frac{1}{2} \left(\frac{Z_0}{R_p} \right) \right]. \tag{8}$$

The insertion loss of two imperfect ON diodes having series resistance R_s is given [11] by

$$\delta = 40 \log \left[1 + \frac{1}{2} \left(\frac{R_s}{Z_0} \right) \right]. \tag{9}$$

The insertion losses add to give a total insertion loss

$$\delta_\phi = 40 \log \left[1 + \frac{1}{2} \left(\frac{R_s}{Z_0} + \frac{Z_0}{R_p} \right) \right]. \tag{10}$$

3) Power Limitations: A DPDT switch can control average incident power $\overline{P}_i$ given by [12]

$$\overline{P}_i = \frac{\overline{P}_D Z_0}{R_s} \left(1 + \frac{R_s}{2Z_0} \right)^2 \tag{11}$$

in which $\overline{P}_D$ is the average power the diode can dissipate.

The insertion-loss calculations given earlier indicated that the OFF diodes have the same voltages and currents on them as if they were shunted to ground. The peak power a shunt diode can control $\hat{P}_i$ is given [11] by

$$\hat{P}_i = \frac{E_B^2}{8Z_0} \tag{12}$$

in which E_B is the breakdown voltage of the diode.

As long as the regions of large phase error and high insertion loss are avoided, these power equations will be valid.

4) Broad Bandwidth: The switched-line phase shifter is a time-delay device. Phase shift will be proportional to frequency. Wide bandwidth may be achieved by using a Schiffman phase shifter [13] in one of the transmission paths. The phase shift of the Schiffman coupled section is a linear function of frequency plus a sinusoidal function of frequency. When l_1 is selected so that it is parallel to the center portion of the Schiffman curve on the ϕ–ω plot, then a relatively constant phase shift is available over a significant bandwidth. Care must be taken that neither line intersects multiples of 180° over the band of interest or large phase errors and insertion loss will occur, as discussed previously in 1).

B. Reflection Phase Shifters

A reflection phase shifter can be made of a shunt diode with a short circuit behind it, as shown in Fig. 1, a series diode with an open circuit behind it, or a lumped circuit including diode parasitics terminating the line. The switches backed up by lengths of transmission line have the advantage that they are time-delay devices giving wide instantaneous bandwidth for phased-array radars, while the lumped-circuit versions can be made to give constant phase shift over octave or wider bandwidths.

A source of error exists for the reflection phase shifter that is not present for the others. Mismatches intervening between the terminating impedance and the perfect circulator or 3-dB coupler contribute large phase errors

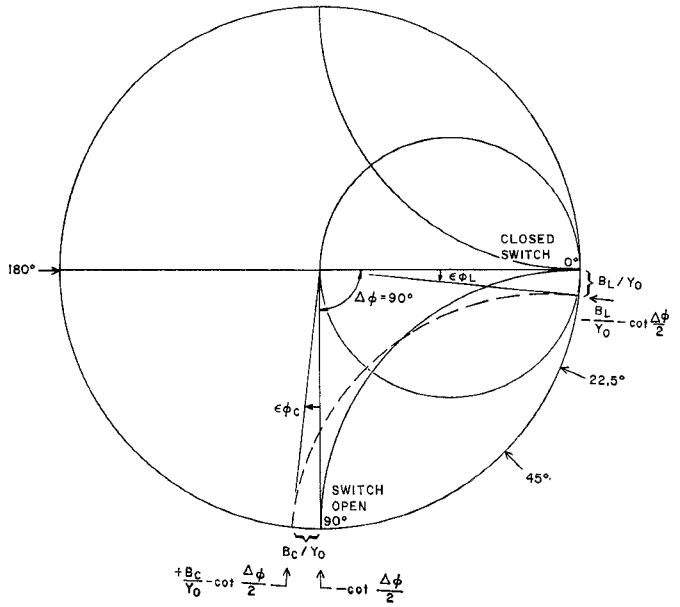

Fig. 5. Admittance of a switching diode with parasitics in a 90° reflection phase shifter.

[14]. The maximum phase error ϵ_ϕ for an intervening mismatch of Γ_M in front of a reflector Γ_x is given by

$$\epsilon_\phi = \pm (1 + 3|\Gamma_x| - \tfrac{1}{4}\sin\pi|\Gamma_x|)\sin^{-1}\left|\frac{\Gamma_M}{\Gamma_x}\right|. \quad (13)$$

For low-loss phase shifters $|\Gamma_x| = 1$ and

$$\epsilon_\phi = \pm 4\sin^{-1}|\Gamma_M|. \quad (14)$$

An intervening mismatch having a VSWR of 1.2 will give $\epsilon_\phi = \pm 20.8°$. Therefore, it is very important to have no mismatches between the circulator (or 3-dB coupler) and the reflection element(s). This error is very closely given by

$$\epsilon_\phi = \pm 100°(\rho - 1) \quad (15)$$

in which ρ is VSWR.

Caution must also be used in selecting a circulator or 3-dB coupler because the finite isolation is caused by internal reflections in the coupling device. For example, a circulator having 20-dB isolation has an internal voltage reflection coefficient of 0.1, which gives $\pm 22.8°$ maximum phase error; 30-dB isolation gives a $\pm 7.2°$ maximum phase error; and 40-dB gives $\pm 2.3°$. It is possible that by carefully arranging phases, the maximum phase error can be avoided.

1) Time-Delay Phase Shifter: The time-delay phase shifter shown in Fig. 1 has the advantage that it tends to have the instantaneous wide bandwidth needed for pulsed phased-array radars. The normalized admittance of the termination may be considered as shown in Fig. 5. The admittance is shown as it would be measured in the plane of the diode switch. A perfect switch has infinite admittance when closed, giving $\infty + j\infty$ on the Smith chart for all lengths of line behind it. When the perfect switch is opened, all that is seen is the admittance of the length of line behind it $\Delta l/2$, which is given by

$$Y/Y_0 = -j\cot[2\pi(\Delta l/2)/\lambda] = -j\cot\frac{\Delta\phi}{2}. \quad (16)$$

The circular arc shown in Fig. 5 shows the admittance that would be traced out by a perfect p-i-n diode switch as current is varied between 0 and ∞ for 90° phase shift. Forward bias on the diode corresponds to closed switch and reverse bias to switch open. The switch open admittances for other phase shifts are indicated on the figure. The switch closed admittances would all be at $\infty + j\infty$.

A typical nonperfect diode switch will be inductive for conduction and capacitive for reverse bias. The inductive susceptance will cause the error shown in Fig. 5 as $\epsilon_{\phi L}$, while the capacitive susceptance will cause the error shown as $\epsilon_{\phi C}$. Proper selection of diode parasitics can permit these errors to cancel out (as illustrated in Fig. 5).

The insertion loss of a reflection diode phase shifter is normally dominated by the diode impedance at forward bias R_s. At reverse bias the structure normally has a higher VSWR, and a resistor is placed in parallel with the diode to make the VSWR equal in both phase states [15], [16].

The insertion loss is given by

$$\delta_\phi = 20\log\left(1 + 2\frac{R_s}{Z_0}\right). \quad (17)$$

The maximum peak power a time-delay reflection phase shifter can control is given [12] by

$$\hat{P}_i = \frac{E_B^2}{32Z_0\sin^2\left(\frac{\Delta\phi}{2}\right)} \quad (18)$$

and the maximum average power for most practical conditions is given by

$$\overline{P}_i = \frac{\overline{P}_D Z_0}{4R_s}. \quad (19)$$

2) Wide-Band Reflection Phase Shifter: For wide-band phase shifting, the diode(s) is(are) connected to the circulator (3-dB coupler) without a length of transmission line behind it(them). A perfect diode switch will be 0 Ω when closed and ∞ Ω when open. These impedances are 180° apart on the Smith chart and therefore give $\Delta\phi = 180°$. If the short circuit is considered the reference, the open circuit is equivalent to a short circuit $\lambda/4$ away,

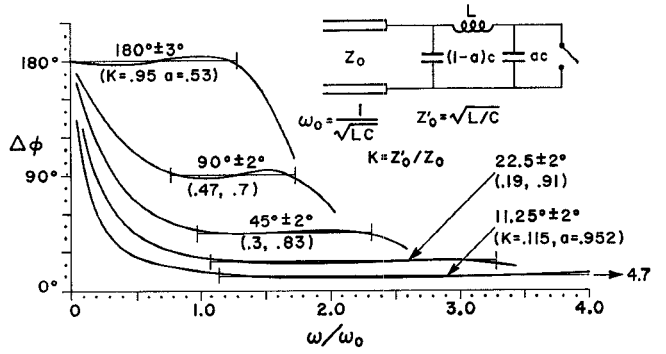

Fig. 6. Wide-band performance of lumped-element diode reflection phase shifter.

and the effective round trip to the effective short circuit gives a $\lambda/2$ phase delay or 180°.

An imperfect diode was considered by Garver [15] for the 180° bit, and has subsequently been widely adopted for the 180° bit in most digital diode phase shifters reported to date [4], [17]. The bandwidth for the 180° bit is limited by the circulator or 3-dB coupler.

The phase shift in general is given by

$$\Delta\phi = 2\left[\tan^{-1}\left(\frac{X_F}{Z_0}\right) - \tan^{-1}\left(\frac{X_R}{Z_0}\right)\right] \tag{20}$$

in which X_F and X_R are the diode reactances at forward and reverse bias. Fig. 6 gives design and performance information for a number of commonly used phase shifts. The term a is that portion of total diode capacitance attributed to the junction. For $\pm 2°$ error, the narrowest bandwidth (for 90°) is wider than an octave. The circuit elements for realizing these phase shifts can be calculated by rearranging the equations given in Fig. 6:

$$C = \frac{1}{Z_0'\omega_0} \qquad L = \frac{Z_0'}{\omega_0}.$$

As an example of using Fig. 6, consider making a phase-shift bit of $45 \pm 2°$ working from 1 to 2 GHz and terminating a transmission line having $Z_0 = 50\ \Omega$. The following calculations would be made.

$$\omega_0 = 2\pi \times 10^9$$

$$Z_0' = kZ_0 = (0.3)(50) = 15\ \Omega$$

$$L = \frac{Z_0'}{\omega_0} = \frac{15}{2\pi \times 10^9} = 2.4\ \text{nH}$$

$$C = \frac{1}{Z_0'\omega_0} = \frac{1}{(15)(2\pi \times 10^9)} = 10.6\ \text{pF}$$

$$C_D = aC = (0.83)(10.6\ \text{pF}) = 8.8\ \text{pF}$$

$$C_C = (1 - a)C = (0.17)(10.6\ \text{pF}) = 1.8\ \text{pF}.$$

Using $ABCD$ matrices, the power and insertion-loss equations for the constant-phase reflection phase shifter have been derived [12].

$$\hat{P}_i = \frac{E_B^2}{32Z_0}\left\{\left[1 - a\left(\frac{\omega}{\omega_0}\right)^2\right]^2 + \left[\frac{1}{k} - (1 - a)\left(\frac{\omega}{\omega_0}\right)\right]^2\left(\frac{\omega}{\omega_0}\right)^2\right\} \tag{21}$$

$$\overline{P}_i = \frac{\overline{P}_D}{4R_sY_0}\left\{k^2\left(\frac{\omega}{\omega_0}\right)^2 + \left[1 - (1 - a)\left(\frac{\omega}{\omega_0}\right)^2\right]^2\right\} \tag{22}$$

$$\delta_\phi = 10 \log\left[\frac{1}{1 - \overline{P}_D/\overline{P}_i}\right]. \tag{23}$$

The insertion-loss equation obtains $\overline{P}_D/\overline{P}_i$ from (22).

C. Loaded-Line Phase Shifters

1) General: The normalized $ABCD$ matrix of two normalized susceptances B_N shunting a transmission line and separated by $\theta = 2\pi l/\lambda$, as shown in Fig. 1, is given by

$$\begin{vmatrix} A & B \\ C & D \end{vmatrix}_N = \begin{vmatrix} 1 & 0 \\ jB_N & 1 \end{vmatrix}\begin{vmatrix} \cos\theta & j\sin\theta \\ j\sin\theta & \cos\theta \end{vmatrix}\begin{vmatrix} 1 & 0 \\ jB_N & 1 \end{vmatrix} = \begin{vmatrix} \cos\theta - B_N\sin\theta & j\sin\theta \\ j[2B_N\cos\theta + (1 - B_N^2)\sin\theta] & \cos\theta - B_N\sin\theta \end{vmatrix}. \tag{24}$$

The transmission coefficient of a normalized $ABCD$ matrix is given by

$$S_{21} = \frac{2}{A + B + C + D} = \frac{1}{[\cos\theta - B_N\sin\theta] + j\left[B_N\cos\theta + \left(1 - \frac{B_N^2}{2}\right)\sin\theta\right]}. \tag{25}$$

The phase ϕ of the loaded transmission line section is given by

$$\phi = \tan^{-1}\left[-\frac{B_N\cos\theta + \left(1 - \frac{B_N^2}{2}\right)\sin\theta}{\cos\theta - B_N\sin\theta}\right] = \tan^{-1}\left[-\frac{B_N + (1 - \tfrac{1}{2}B_N^2)\tan\theta}{1 - B_N\tan\theta}\right]. \tag{26}$$

Positive phase corresponds to phase advance, and negative phase to phase delay. Since the $\tan^{-1}$ function is normally taken between $\pm\pi/2$, the phase delay can be

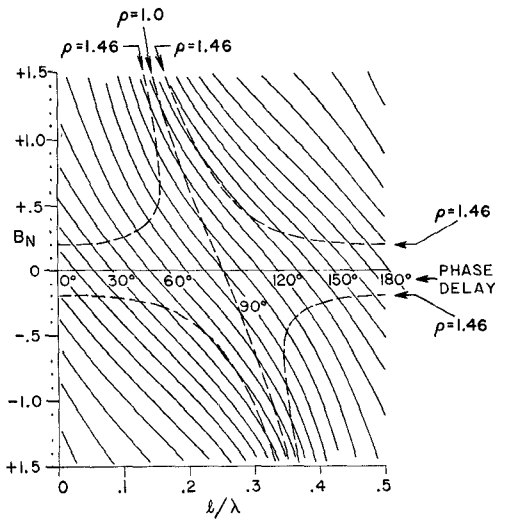

Fig. 7. Loaded-line phase shifts and VSWR limits.

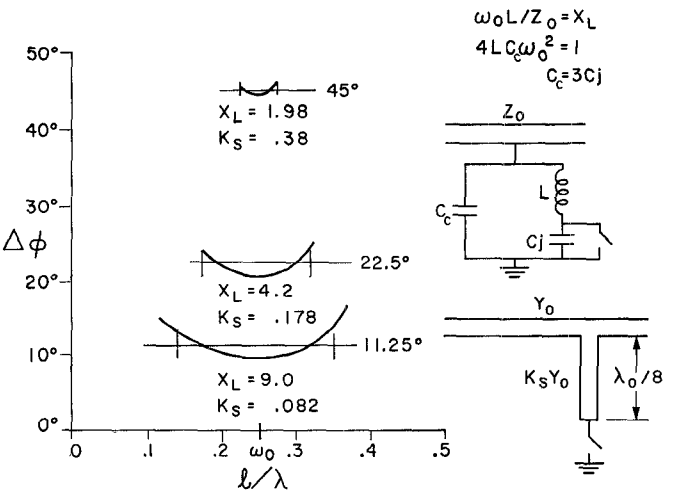

Fig. 8. Frequency dependence of loaded-line phase shifters designed for maximum bandwidth. Curves stop at $\rho = 1.46$. Ticks indicate end of $\pm 2°$ range.

represented by

$$\phi_D = \pi + \tan^{-1}\left[\frac{B_N + (1 - \frac{1}{2}B_N^2)\tan\theta}{1 - B_N \tan\theta}\right]. \quad (27)$$

This phase delay is shown graphically in Fig. 7.

Since the structure of Fig. 1 is lossless, the magnitude of the input reflection coefficient is given by

$$|S_{11}| = \sqrt{1 - |S_{21}|^2} = \sqrt{1 - \frac{1}{1 + B_N^2(\cos\theta - \frac{1}{2}B_N \sin\theta)^2}} \quad (28)$$

and the input VSWR ρ is given by

$$\rho = \frac{1 + |S_{11}|}{1 - |S_{11}|}. \quad (29)$$

The magnitude of VSWR that can be tolerated is determined by the amount of phase uncertainty that is caused by two interacting VSWRs. Phase uncertainty is given [18] by

$$\epsilon_\phi = \pm \sin^{-1}[|\Gamma_1||\Gamma_2|] \quad (30)$$

in which Γ_1 and Γ_2 are the reflection coefficients of the interacting discontinuities. When both phase bits are allowed to have the same reflection coefficient Γ, the error is given by

$$\epsilon_\phi = \pm \sin^{-1}|\Gamma|^2 \quad (31)$$

or

$$|\Gamma| = \sqrt{\sin \epsilon_\phi}. \quad (32)$$

Allowing each bit to have $\pm 2°$ phase error gives

$$\Gamma = 0.187$$

or

$$\rho = 1.46.$$

Using (28) and (29), B_N and θ are calculated giving $\rho = 1.46$, which gives the dashed curves shown superimposed on Fig. 7.

The practical range of phase in Fig. 7 is bounded by the dashed curves for $\rho = 1.46$. A phase-shift range of 75° is available over more than a 2:1 range in values of l/λ.

2) Switching with Stubs: Some practical circuits for making loaded-line phase shifters are shown in Fig. 8. Using the stubs, the normalized admittance of the stubs for perfect open-circuit switches B_{NO} is given by

$$B_{NO} = K_s \tan K_\theta \theta. \quad (33)$$

When the switches are closed, the normalized admittance of each stub B_{NS} is given by

$$B_{NS} = -K_s \cot K_\theta \theta. \quad (34)$$

When (33) and (34) are alternately put into (29), the difference in phases is the phase shift that is shown for various values of K_s and K_θ in Fig. 8. The curves stop when either phase has a VSWR of 1.46. The parameters were selected to give the $\pm 2°$ range, but the VSWR became too high with the higher phase shifts to reach the $\pm 2°$ points. The 45° phase shift is available over about 25-percent bandwidth, while 22.5° is available over an octave bandwidth, and 11.25° phase shift is available over almost two octaves bandwidth.

Both circuits of Fig. 8 tend to have the same curvature. Neither circuit could give more than the single-ripple responses shown in Fig. 8. It is possible that an analysis permitting the diodes to be different could permit wider bandwidth than that calculated from Fig. 8. It should be noted as a practical matter that seldom can Z_0 be made much outside of the 25–100-Ω range.

Thus when Z_0 is 25 Ω, $K_s = 0.25$ is a practical lower limit. Only at the expense of unusual characteristic impedances can wide bandwidths be realized using the simple circuits shown in Fig. 8.

Computer simulations have shown that the widest bandwidth is centered about $l/\lambda = 0.25$ when the stubs are $\lambda/8$ long. At that point, the B_N versus l/λ lines for open and short are parallel, and (27) reduces to

$$\phi_D = \pi - \tan^{-1}\left[\frac{1 - \frac{1}{2}B_N^2}{B_N}\right]. \tag{35}$$

Open-circuit diodes will introduce a positive susceptance B_N and a large phase delay ϕ_{DO}, while short-circuit diodes will give a negative susceptance B_N with small phase delay ϕ_{DS}. The phase shift is given by

$$\Delta\phi = \phi_{DO} - \phi_{DS} = 2\tan^{-1}\left[\frac{B_N}{1 - \frac{1}{2}B_N^2}\right] \tag{36}$$

which gives the values for K_s at $l/\lambda = 0.25$. in Fig. 8. For example, the 22.5° curve shows 20.5°, which gives $B_N = 0.178 = K_s$. (The susceptance of a $\lambda/8$ stub is $\pm jK_sY_0$.)

3) Switching with Lumped-Element Diodes: Requiring that the susceptance curves be parallel at $l/\lambda = 0.25$ and that $B_{NO} = B_{NS}$, the circuit-element values for the lumped-element diodes of Fig. 8 can be calculated. Computer calculations of a figure similar to Fig. 8 showed the same properties (bandwidth, centering of $l/\lambda = 0.25$).

The normalized shunt susceptance of each diode when the switch SW is closed, B_{NS}, is given by

$$B_{NS} = \frac{\omega(1-a)C}{Y_0} - \frac{1}{Y_0\omega L}. \tag{37}$$

The normalized shunt susceptance of each diode when the switch SW is open, B_{NO}, is given by

$$B_{NO} = \frac{\omega(1-a)C}{Y_0} - \frac{1}{Y_0\omega L - \frac{Y_0}{\omega aC}}. \tag{38}$$

Matching the slopes at ω

$$\frac{\partial B_{NS}}{\partial \omega} = \frac{\partial B_{NO}}{\partial \omega}$$

gives

$$a = \frac{1}{3\omega^2 LC} = \frac{1}{3}\frac{\omega_0^2}{\omega^2} \tag{39}$$

using the definition for $\omega_0^2 = 1/LC$ as given in Fig. 6.

Setting up the equation

$$B_{NO} = -B_{NS}$$

produces

$$\frac{\omega_0^2}{\omega^2} = \frac{12}{7}$$

and

$$a = \frac{4}{7}.$$

Requiring the relationship $B_{NS} = -B_N$ produces

$$\frac{1}{\omega L Y_0} = \frac{4}{3}B_N \tag{40}$$

$$\frac{\omega C}{Y_0} = \frac{7}{9}B_N \tag{41}$$

in which B_N may be obtained from (36) or from $K_s = B_V$ in Fig. 8. The term ω in (40) and (41) is given for the frequency of $\lambda/4$ spacing between diodes.

4) Narrow-Band Perfect-Match Phase Shifters: The previous analysis has been for $\lambda/4$ spacing between diodes because that spacing gives the widest bandwidth and has been the most widely used in practice. However, a phase shift greater than 45° is not possible without causing excessively high VSWR. Higher amounts of phase shift can be obtained by having $B_N = 0$ in one bias state and B_N equal to some positive number in the other bias state. The spacing between the diodes is adjusted so that $\rho = 1.0$ as in Fig. 7. Setting the relationship $|S_{11}| = 0$ in (28) gives

$$\tan\theta = \frac{2}{B_N}. \tag{42}$$

Substituting (42) into (27) produces

$$\phi_D = \pi - \tan^{-1}\left[\frac{2}{B_N}\right]. \tag{43}$$

The phase delay ϕ_{DN} of the line with no diode shunting it ($B_N = 0$) is exactly equal to its electrical length, giving

$$\phi_{DN} = \theta = \tan^{-1}\left[\frac{2}{B_N}\right]. \tag{44}$$

The increased phase delay due to switching the diodes into the circuit is given by

$$\begin{aligned}\Delta\phi &= \phi_D - \phi_{DN} \\ &= \pi - \tan^{-1}\left[\frac{2}{B_N}\right] - \tan^{-1}\left[\frac{2}{B_N}\right] \\ &= \pi - 2\tan^{-1}\left[\frac{2}{B_N}\right]\end{aligned} \tag{45}$$

which reduces to

$$B_N = 2\tan\left(\frac{\Delta\phi}{2}\right). \tag{46}$$

Or, using (44), (45) can be reduced to

$$\Delta\phi = \pi - 2\theta \tag{47}$$

which gives

$$\theta = \frac{\pi}{2} - \frac{\Delta\phi}{2} = \frac{2\pi l}{\lambda}. \tag{48}$$

Equations (46) and (48) give the susceptance and spacing for a narrow-band perfectly matched loaded-line phase shifter.

At midband the power limitations and insertion loss of the loaded-line phase shifter [12] are as follows:

$$\hat{P}_i = \frac{E_B^2}{4Z_0}\left[1 + \frac{K_s^2}{4}\right] \tag{49}$$

$$\overline{P}_i = \frac{\overline{P}_D}{2R_s Y_0}\left[1 + \frac{4}{K_s^2}\right] \tag{50}$$

$$\delta_\phi = 20 \log \left[\frac{1 + \dfrac{4R_s Y_0}{4}}{1 + \dfrac{4}{K_s^2}}\right]. \tag{51}$$

D. High-Pass Low-Pass Phase Shifter

A low-pass filter comprised of series inductors and shunt capacitors provides phase delay to signals passing through it, and a high-pass filter comprised of series capacitors and shunt inductors provides phase advance. By arranging diode switches to permit switching between low pass and high pass, it is possible to make a phase shifter that is smaller than the other types and with a bandwidth almost as good as the lumped-element reflection phase shifter.

1) General: The normalized $ABCD$ matrix for the elements of Fig. 1 switched in the low-pass state is given by

$$\begin{vmatrix} A & B \\ C & D \end{vmatrix}_N = \begin{vmatrix} 1 & jX_N \\ 0 & 1 \end{vmatrix} \begin{vmatrix} 1 & 0 \\ jB_N & 1 \end{vmatrix} \begin{vmatrix} 1 & jX_N \\ 0 & 1 \end{vmatrix}$$

$$= \begin{vmatrix} 1 - B_N X_N & j(2X_N - B_N X_N^2) \\ jB_N & 1 - B_N X_N \end{vmatrix}. \tag{52}$$

The transmission term of the scattering matrix S_{21} of the normalized $ABCD$ matrix is given by

$$S_{21} = \frac{2}{A + B + C + D}$$

$$= \frac{2}{2(1 - B_N X_N) + j(B_N + 2X_N - B_N X_N^2)}. \tag{53}$$

The transmission phase ϕ is given by

$$\phi = \tan^{-1}\left[-\frac{B_N + 2X_N - B_N X_N^2}{2(1 - B_N X_N)}\right]. \tag{54}$$

This phase is shown in Fig. 9 for a range of B_N (converted to normalized shunt reactance) and X_N. When both B_N and X_N change signs, the phase remains the same but changes sign; thus the phase shift $\Delta\phi$ caused by switching between low pass and high pass is twice

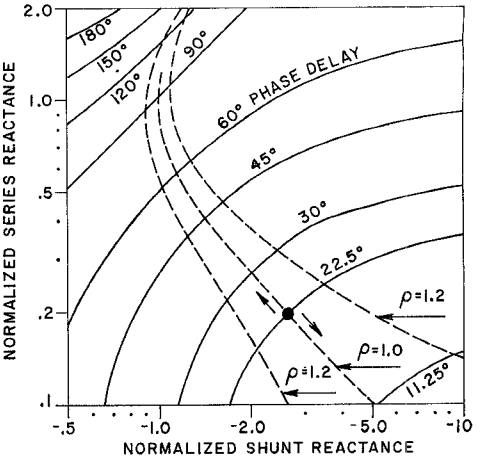

Fig. 9. Phase shift of lumped-element low-pass T-section phase-shift paths.

(54), giving

$$\Delta\phi = 2 \tan^{-1}\left[-\frac{B_N + 2X_N - B_N X_N^2}{2(1 - B_N X_N)}\right]. \tag{55}$$

Assuming the phase shifter to be lossless, the reflection coefficient S_{11} is given by

$$|S_{11}| = \sqrt{1 - |S_{21}|^2}. \tag{56}$$

The phase shifter will be perfectly matched when the equation $|S_{21}| = 1$ is satisfied. Under conditions of match, (53) reduces to

$$B_N = \frac{2X_N}{X_N^2 + 1}. \tag{57}$$

Substitution of (57) into (55) gives

$$\Delta\phi = 2 \tan^{-1}\left[\frac{2X_N}{X_N^2 - 1}\right] \tag{58}$$

which reduces to

$$X_N = \tan\left(\frac{\Delta\phi}{4}\right). \tag{59}$$

Using (59) in (57) gives

$$B_N = \sin\left(\frac{\Delta\phi}{2}\right). \tag{60}$$

A pi section filter instead of a T would exchange (59) and (60) (X_N and B_N). Fig. 9 would also show the phase, but would be for susceptances instead of reactances and the coordinates would be exchanged.

The frequency dependence of the phase shifter may be studied with the aid of Fig. 9. For example, a 45° phase shifter will have $X_N = 0.199$ and $B_N = 0.382$ using (59) and (60). These two values fall at the intersection of $\rho = 1.0$ and 22.5° in Fig. 9. As frequency is increased in the low-pass state, the series reactance increases proportional to frequency and the shunt

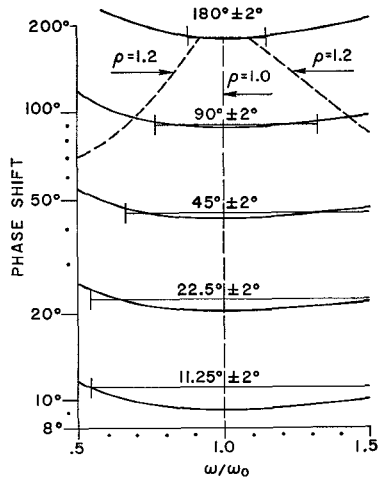

Fig. 10. Frequency dependence of lumped-element low-pass high-pass phase shifters.

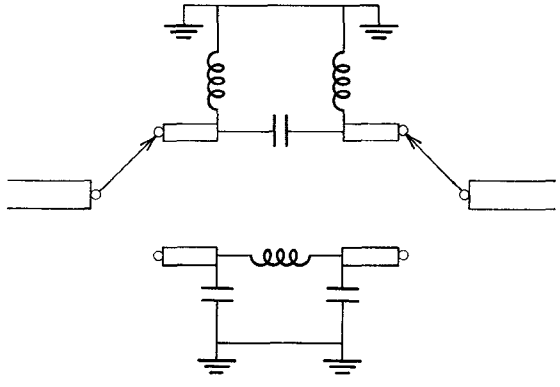

Fig. 11. Practical layout of low-pass high-pass phase shifter.

reactance decreases inversely proportional to frequency. The intersection of the two reactances moves towards the upper left corner of the figure at 45° off vertical, closely following the $\rho = 1.0$ curve and increasing phase delay. On the other hand, in the high-pass state, the series reactance decreases with increasing frequency and the shunt reactance increases. The intersection of the two reactances moves towards the lower right corner of the figure, again closely following the $\rho = 1.0$ curve but now decreasing phase advance. The net effect is that the phase shifter tends to stay matched as frequency is increased, and phase delay increase in the low-pass state is compensated for by phase advance lost in the high-pass state.

The frequency dependence of the high-pass low-pass phase shifter is shown in Fig. 10. Low VSWR is easily obtained. A phase shift of $90° \pm 2°$ is obtainable over almost an octave, while the smaller phase shifts are available over more than an octave. If bandwidth is limited to an octave, $90° \pm 4$ percent is possible and the smaller phase shifts have errors of ± 3 percent.

A more practical embodiment of the high-pass low-pass phase shifter may be as shown in Fig. 11. Two SPDT switches are required instead of three, and parasitics due to OFF diodes and lines are more easily accounted and compensated for.

The bandwidth of the large phase-shift bits may be improved by using more elements in the high-pass and low-pass circuits.

2) Power Limitations and Insertion Loss: The power limitations of the phase shifter as shown in Fig. 11 will be the same as for the switched-line phase shifter as given in (11) and (12). The insertion loss contributed by the diodes is given by (10). Some insertion loss will also be contributed by the finite Q's of the circuit elements, and it may be necessary to "spoil" the Q in some of the elements to keep the insertion loss the same in both phase states. Another solution would be to use a T circuit for high pass and a pi circuit for low pass.

Some caution must be exercised to avoid the regions of high insertion loss and high phase error as encountered in the switched-line shifter and as exemplified in Fig. 3. Recall [11] that the attenuation α of a series diode is given by

$$\alpha = 10 \log \left[(1 + \tfrac{1}{2} R_N)^2 + (\tfrac{1}{2} X_N)^2 \right] \tag{61}$$

in which the normalized impedance of the diode is $R_N + jX_N$. A 20-dB reactively limited isolation will have $X_N = -20$ and 10 dB, $X_N = -6$. The normalized reactance X_N of an open-circuit line of length θ is given by

$$X_N = -\cot \theta. \tag{62}$$

The 20-dB switch appears to be an electrical length of 2.9° of open-circuit line, and the 10-dB switch appears to be 9.5°. Recall from Section A-2 that 180° length in the OFF line must be avoided to avoid insertion-loss and phase-error spikes. Since one diode is at each end of each line, the 20-dB diodes add 5.8° to the OFF line and the 10-dB diodes add 19°. Therefore, phase delays of 174.2°–161° must be avoided in the OFF lines depending on SPST diode isolation. It can be seen from Fig. 9 that such large phase delays are not normally encountered with simple T or pi circuits in the high-pass low-pass phase shifter. But phase advances of 5.8°–19° must also be avoided to avert the troublesome spikes. These advances are normally encountered with the smaller phase-shift bits. The problem of too little phase delay in one path may be corrected by adding short lengths of transmission line between the T or pi sections and the diode switches, as shown in Fig. 11.

Conclusions

All four types of phase shifters can give octave bandwidth for low values of phase shift. The phase-shifter circuit least likely to give wide bandwidth is the loaded-line type. The type next most difficult to work with is the reflection type, because of the strict requirements on intervening mismatches to prevent phase errors. The switched-line phase shifter is most satisfactory for constant time-delay phase shifting, but the

region $2\pi l/\lambda = 180°$ must be avoided in either path length. Thus, if the phase shifter were to be used in a phased array of much length and large sweep angle, many 90° bits would have to be used for the longer time-delay paths. When the switched-line phase shifter is used with Schiffman constant phase-delay lines, the long lengths of the lines constrain the constant phase-shift bandwidth to about $\frac{1}{2}$ octave. The new lumped-element high-pass low-pass phase shifter gives a very good constant phase shift for $\Delta\phi \leq 90°$. A practical octave bandwidth constant phase-shift phase shifter would use the new type phase shifters for all but the 180° bit, which could be a reflection device made using a very carefully matched quarter-wavelength 3-dB coupler and a pair of diodes.

References

[1] E. M. Rutz and J. E. Dye "Frequency translation by phase modulation," in *1957 IRE WESCON Conv. Rec.*, pt. 1, pp. 201–207.

[2] W. A. Little, J. Yuan, and C. C. Snellings, "Hybird integrated circuit digital phase shifters," in *1967 IEEE Int. Solid-State Circuits Conf. Dig.*, pp. 58–59.

[3] A. E. Cohen, "Some aspects of microwave phase shifters using varactors," in *1962 Proc. 6th Nat. Conv. Military Electron.*, pp. 328–332.

[4] B. W. Battershall and S. P. Emmons, "Optimization of diode structures for monolithic integrated circuits," *IEEE Trans. Microwave Theory Tech.*, vol. MTT-16, pp. 445–450, July 1968.

[5] H. N. Dawirs and W. G. Swarner, "A very fast, voltage-controlled, microwave phase shifter," *Microwave J.*, pp. 99–107, June 1962.

[6] J. F. White, "High power, *p-i-n* diode controlled, microwave transmission phase shifters," *IEEE Trans. Microwave Theory Tech.*, vol. MTT-13, pp. 233–242, Mar. 1965.

[7] P. Onno and A. Plitkins, "Lumped constant, hard substrate, high power phase shifters," presented at the IEEE MIC (Materials and Design) Seminar, Monmouth College, West Long Branch, N. J., June 1970.
——, "Miniature multi-killowatt PIN diode MIC digital phase shifters," in *1971 IEEE-GMTT Int. Microwave Symp. Dig.*, Catalog no. 71 C25-M, pp. 22–23.

[8] J. D. Young, "Integrated circuitry for electronic beam steering of wide-band slot antennas," Ohio State Univ., Columbus, Contract AF 33(657)-10386, AD 474 650, Nov. 10, 1965.

[9] R. G. Stewart and M. N. Guiliano, "*X*-band integrated diode phase shifters," in *1968 IEEE GMTT Int. Microwave Symp. Dig.*, pp. 147–154.

[10] E. J. Wilkinson, L. I. Parad, and W. R. Connerney, "An *X*-band electronically steerable phased array," *Microwave J.*, pp. 43–48, Feb. 1964.

[11] R. V. Garver, "Theory of TEM diode switching," *IRE Trans. Microwave Theory Tech.*, vol. MTT-9, pp. 224–238, May 1961.

[12] ——, "Microwave diode control devices (switches, limiters, attenuators, and phase shifters)," Harry Diamond Labs., Washington, D. C., Final Rep., in press.

[13] C. H. Grauling and D. B. Geller, "A broad-band frequency translator with 30-dB suppression of spurious sidebands," *IEEE Trans. Microwave Theory Tech.* (Corresp.), vol. MTT-18, pp. 651–652, Sept. 1970.

[14] R. V. Garver, D. Bergfried, S. Raff, and B. O. Weinschel, "Errors in S_{11} measurements due to residual SWR of the measurement equipment," in *1971 IEEE-GMTT Int. Microwave Symp. Dig.*, Catalog no. 71 C25-M, pp. 38–39; also *IEEE Trans. Microwave Theory Tech.*, vol. MTT-20, pp. 61–69, Jan. 1972.

[15] R. V. Garver, "Broadband binary 180° diode phase modulators," *IEEE Trans. Microwave Theory Tech.*, vol. MTT-13, pp. 32–38, Jan. 1965.

[16] ——, "360° varactor linear phase modulator," *IEEE Trans. Microwave Theory Tech.*, vol. MTT-17, pp. 137–147, Mar. 1969.

[17] R. W. Burns and L. Stark, "PIN diode advance high-power phase shifting," *Microwaves*, pp. 38–48, Nov. 1965.

[18] E. N. Phillips, "The uncertainties of phase measurement," *Microwaves*, pp. 14–21, Feb. 1965.

Equivalent Network for Interacting Thick Inductive Irises

TULLIO E. ROZZI, MEMBER, IEEE

***Abstract*—An equivalent network is presented for symmetric inductive irises in rectangular waveguides. This model exactly describes the effects of finite thickness and interaction via higher order modes due to the presence of neighboring irises, as in practical waveguide filters.**

Manuscript received June 21, 1971; revised September 28, 1971.
The author is with the Philips Research Laboratories, N. V. Philips' Gloeilampenfabrieken, Eindhoven, The Netherlands.

Introduction

THE NECESSITY of finding an exact equivalent network representation for inductive irises having finite thickness and possibly interacting via higher order modes arises in the design of high-precision waveguide filters. Current design practice assumes the irises as infinitely thin and noninteracting. A thickness cor-